

Role of Ligand Bending in the Photodissociation of O₂ vs CO-heme: A Time-Dependent Density Functional Study

Filippo De Angelis,^{*,†} Roberto Car, and Thomas G. Spiro

Department of Chemistry, Princeton University, Princeton, New Jersey 08544

Received July 18, 2003; E-mail: filippo@thch.unipg.it

We report a facile pathway for de-excitation of photoexcited O₂-heme and the absence of such a pathway for CO-heme. This pathway can account for the dramatic difference in photodissociation quantum yields for O₂ and CO adducts of heme proteins.¹

Heme proteins are biological receptors of the gaseous XO molecules (X = C, N, O), and the dynamics of their binding is of longstanding interest. Rebinding dynamics are conveniently studied by inducing ligand dissociation with a light pulse, but the XO photodissociation characteristics differ dramatically. The dissociation quantum yield is unity for CO but is much lower for NO and O₂. It had been uncertain how much of the inefficient dissociation is attributable to fast geminate recombination and how much to internal conversion processes, but recent measurements by Ye et al.¹ established the zero-time quantum yields to be 50 and 28% for NO and O₂ adducts of myoglobin (Mb), in contrast to the 100% yield of MbCO. This variation correlates with adduct geometry; the Fe–X–O bond angle is approximately 180, 145, and 120° for X = C, N, and O. The geometry can be rationalized on the basis of the degeneracy of the FeXO π* orbitals in the linear geometry. When these orbitals are singly (NO) or doubly (O₂) occupied, this degeneracy is lifted via a bending distortion,² as detailed in the vibrational interaction theory of Bersuker and Stavrov.³ Ye et al.¹ suggested that this theory might also account for the variation in quantum yield; if photoexcitation favors bending, then the linear FeCO might be more prone to photodissociation than the already bent FeNO and FeO₂. They further suggested that a side-on isomer of FeO₂, which has been proposed to be the low-temperature photolysis product of an Fe(II)porphyrin–O₂ adduct,⁴ might contribute to the low MbO₂ dissociation quantum yield and might account for the observation⁵ of an unphotolyzable fraction at 10 K.

In the course of investigating protein effects on CO and O₂ binding in Mb at a full quantum chemical level,⁶ we found a side-on O₂ isomer, which is stabilized by hydrogen bonding,^{6,7} only 10.7 kcal mol⁻¹ above the more stable end-on isomer. Motivated by this result, we sought to evaluate the excited-state geometry dependence of an (imidazole)Fe(II)porphine (Im)FeP model with bound CO or O₂ ligands (Supporting Information) by means of time-dependent DFT calculations,⁸ using the B3LYP⁹ functional and a LANL2DZ¹⁰ basis set, along with the corresponding pseudopotential for the iron atom, as implemented in the Gaussian 98 program package.¹¹ DFT calculations on heme models have given a good account of the XO adduct geometries¹² and vibrational frequencies.^{12b} Figure 1 gives structural parameters for the computed equilibrium geometries of the end-on and side-on isomers of the O₂ adducts optimized, without any symmetry constraints, at the B3LYP/LANL2DZ level. Constrained geometry optimizations were then performed at selected values of the Fe–X–O angle and of

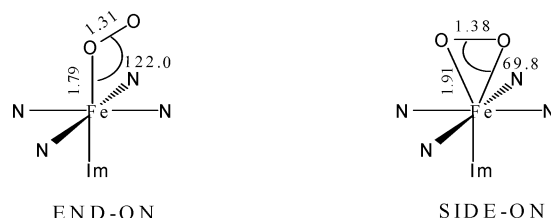


Figure 1. Fe–O–O bond distances and angles (Å, degree) in the optimized end-on and side-on isomers of (Im)FeO₂. The end-on parameters agree well with the X-ray structure of MbO₂¹⁷ and with previous theoretical studies.¹² The side-on isomer shows an elongated O–O distance, similar to that seen in peroxide complexes.

the Fe–X distance, and singlet–singlet vertical excitation energies were computed. The lowest π–π* excitations (Q) were correctly calculated for unconstrained FeCO and FeO₂ as strong transitions at 2.37 and 2.14 eV to be compared to the corresponding experimental values of 2.18 and 2.22 eV, respectively.¹³ In addition, a series of lower-lying FeO₂ transitions of diminishing intensity were computed at 1.27, 1.18, 1.09, and 0.85 eV, in excellent agreement with reported values for oxyhemoglobin.¹³ The lowest-lying singlet excitation corresponds to a transition of negligible intensity computed at 0.41 eV.

Head-Gordon and co-workers¹⁴ recently reported similar computations on the CO model, but focused their analysis on the Fe–C stretching coordinate. They were able to explain photodissociation via population of a repulsive state involving an antibonding Fe_d and CO π* orbital combination, which lies above the photoaccessed Q state but falls below it as the Fe–C bond is stretched. We confirmed this result and found that bending the FeCO moiety did not produce any excited-state crossings. All excited states based on Fe and CO orbitals remained above the Q state, which itself showed negligible variation with the Fe–C–O angle (Supporting Information). Dissociative states falling near higher-lying π–π* excitation, e.g., the Soret band, are of little consequence because of rapid relaxation to Q (Supporting Information).

The situation is entirely different for the O₂ adduct because the Fe_d and O₂ π* orbital combinations are lower in energy and because there is greater mixing of Fe_d and porphyrin π* orbitals. Because of this mixing, the Q state energy drops when the Fe–O bond is stretched (Figure 2), while the energy rises for the various Fe_d–O₂ π* states. Thus, population of the Q state can lead directly to FeO₂ dissociation, without any need for state crossing. On the other hand, multiple crossings are encountered along the Fe–O–O bending coordinate (Figure 3). The ground state displays an energy barrier between the end-on and side-on isomers, while the first excited state displays a complex dependence on the Fe–O–O angle. Its three avoided crossings (marked 1, 2, and 3 in Figure 3) are found to be intersection points when the Fe–O distance dependence is examined; stretching the bond brings the upper and lower surfaces into close contact (Supporting Information). At the same time, a group of low-lying excited states in the end-on isomer rise to the

[†] Present address: Istituto CNR di Scienze e Tecnologie Molecolari (ISTM), Dipartimento di Chimica, Università di Perugia, via Elce di Sotto 8, I-06123, Perugia, Italy.

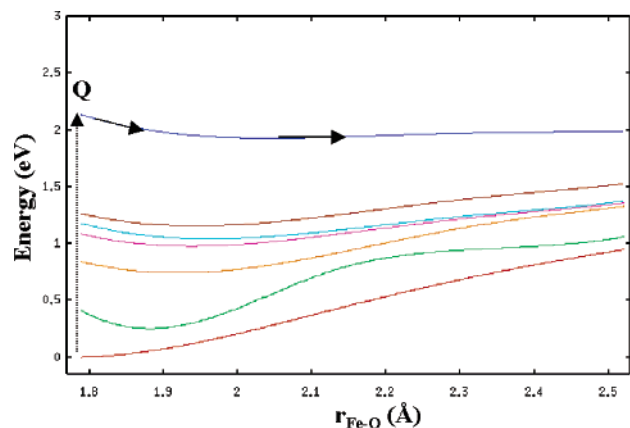


Figure 2. Potential energy curves (eV) of the ground and low-lying excited states of the O_2 complex (end-on isomer) as a function of the Fe–O distance (Å). The Q state is dissociative because of porphyrin and FeO_2 orbital mixing.

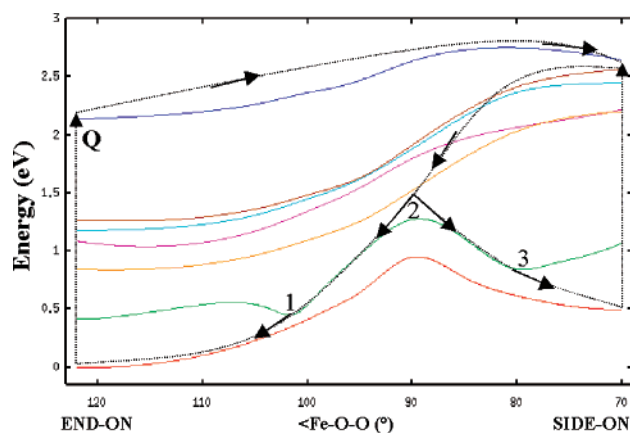


Figure 3. Potential energy curves (eV) of the ground and low-lying excited states of the O_2 complex as a function of the Fe–O–O angle (degree). Arrows mark the suggested pathway of de-excitation from the initially photoexcited Q state to either the end-on or side-on isomers.

vicinity of the Q state in the side-on isomer. The Q state itself rises slightly with diminishing angle, showing a weak maximum 0.4 eV above the end-on energy.

The excited-state profiles in Figure 3 provide a ready pathway (see arrows) for avoidance of photodissociation in the O_2 adduct. Photoexcitation to the Q state would allow access to the side-on isomer, thermal energy being sufficient to surmount the weak barrier. Several states are then close enough to the Q state to funnel energy downward by opening the Fe–O–O angle, populating the first excited state at the avoided crossing 2. Here there is a bifurcation between a pathway leading back to the side-on isomer, via avoided crossing 3, or to the end-on isomer, via avoided crossing 1. The side-on isomer would relax thermally to the end-on isomer, but at low temperature a fraction of the molecules would be trapped in the side-on configuration. Because of the proximity of several states leading downward away from Q (Figure 3), this isomer would readily relax to the ground state, thus providing an explanation for the unphotolyzable Mb O_2 fraction observed at low temperature.⁵

For the end-on isomer, the photolysis probability depends on the rate of progress along the Q state profiles in the stretching and bending directions; the former leads to dissociation, while the latter leads to internal conversion. The full surface along both directions

is undoubtedly complex. Moreover, it depends sensitively on the energy of the side-on isomer. We emphasize that this isomer is stabilized by polar interactions,^{6,7} which are not represented in the present calculations. Thus, the Q state energy may actually decrease along the Fe–O–O bending coordinate in the environment of the protein. It is likely that the observed 28% quantum yield for Mb O_2 photodissociation¹ can be accommodated by this model of de-excitation.

The complex excited-state profiles in Figure 3 can be traced to the strong dependence of the $Fe_d-XO \pi^*$ orbital interactions on the Fe–X–O angle, as analyzed in the classic paper by Hoffman et al.² This dependence exists for FeCO as well as for Fe O_2 , but the excited states arising from these interactions lie at much higher energy for FeCO. The observation that the CO stretching infrared band is polarized parallel to the heme plane within ~ 0.5 ps of MbCO photolysis,¹⁵ which has been cited in favor of a photodissociative bending pathway,¹ may instead reflect the steric interactions of the dissociated CO with the protein residues.¹⁶

Acknowledgment. This work was supported by NIH Grant GM 33576 (to T.G.S.) and by NSF Grant CHE-0121432 (to R.C.).

Supporting Information Available: Geometrical structures and excited-state energy profiles (PDF). This material is available free of charge via the Internet at <http://pubs.acs.org>.

References

- (1) Ye, X.; Demidov, A.; Champion, P. M. *J. Am. Chem. Soc.* **2002**, *124*, 5914.
- (2) Hoffmann, R.; Chen M. M.-L.; Thorn, D. *Inorg. Chem.* **1977**, *16*, 503.
- (3) Bersuker, I. B.; Stavrov, S. S. *Coord. Chem. Rev.* **1988**, *88*, 1.
- (4) Watanabe, T.; Ama, T.; Nakamoto, K. *J. Phys. Chem.* **1984**, *88*, 449.
- (5) (a) Chance, M. R.; Courtney, S. H.; Chavez, M. D.; Ondrias, M. R.; Friedman, J. M. *Biochemistry* **1990**, *29*, 5537. (b) Miller, L. M.; Patel, M.; Chance, M. R. *J. Am. Chem. Soc.* **1996**, *118*, 4511.
- (6) De Angelis, F.; Jarzecki, A.; Car, R. Spiro, T. G., to be submitted for publication.
- (7) Bertran, J.; Ruizlopez, M. F.; Rinalid, D. *THEOCHEM* **1991**, *232*, 337.
- (8) Casida, M. E. In *Recent Advances in Density Functional Methods*; Chon, D. P., Ed.; World Scientific: Singapore, 1995; Vol. I.
- (9) Becke, A. D. *J. Chem. Phys.* **1993**, *98*, 5648.
- (10) Hay, P. J.; Wadt, W. R. *J. Chem. Phys.* **1985**, *82*, 270.
- (11) Frisch, M. J.; Trucks, G. W.; Schlegel, H. B.; Scuseria, G. E.; Robb, M. A.; Cheeseman, J. R.; Zakrzewski, V. G.; Montgomery, J. A., Jr.; Stratmann, R. E.; Burant, J. C.; Dapprich, S.; Millam, J. M.; Daniels, A. D.; Kudin, K. N.; Strain, M. C.; Farkas, O.; Tomasi, J.; Barone, V.; Cossi, M.; Cammi, R.; Mennucci, B.; Pomelli, C.; Adamo, C.; Clifford, S.; Ochterski, J.; Petersson, G. A.; Ayala, P. Y.; Cui, Q.; Morokuma, K.; Malick, D. K.; Rabuck, A. D.; Raghavachari, K.; Foresman, J. B.; Cioslowski, J.; Ortiz, J. V.; Stefanov, B. B.; Liu, G.; Liashenko, A.; Piskorz, P.; Komaromi, I.; Gomperts, R.; Martin, R. L.; Fox, D. J.; Keith, T.; Al-Laham, M. A.; Peng, C. Y.; Nanayakkara, A.; Gonzalez, C.; Challacombe, M.; Gill, P. M. W.; Johnson, B. G.; Chen, W.; Wong, M. W.; Andres, J. L.; Head-Gordon, M.; Replege, E. S.; Pople, J. A. *Gaussian 98*, revision A.7; Gaussian, Inc.: Pittsburgh, PA, 1998.
- (12) (a) Rovira, C.; Kunk, K.; Hutter, J.; Ballone, P.; Parrinello, M. *J. Phys. Chem. A* **1997**, *101*, 8914. (b) Vogel, K. M.; Kozlowski, P. M.; Zgierski, M. Z.; Spiro, T. G. *J. Am. Chem. Soc.* **1999**, *121*, 9915. (c) Rovira, C.; Schulze, B.; Eichinger, M.; Evanseck, J. D.; Parrinello, M. *Biophys. J.* **2001**, *81*, 435. (d) Sigfridsson, E.; Ryde, U. *J. Inorg. Biochem.* **2002**, *91*, 101.
- (13) (a) Makinen, M. W.; Eaton, W. A. *Ann. N.Y. Acad. Sci.* **1973**, *86*, 210. (b) Eaton, W. A.; Hanson, L. K.; Stephens, P. J.; Sutherland, J. C.; Dunn, J. B. R. *J. Am. Chem. Soc.* **1978**, *100*, 4991. (c) Eaton, W. A.; Hofrichter, J. *Methods Enzymol.* **1981**, *76*, 175.
- (14) (a) Dreuw, A.; Dunitz, B. D.; Head-Gordon, M. *J. Am. Chem. Soc.* **2002**, *124*, 12070. (b) Dunitz, B. D.; Dreuw, A.; Head-Gordon, M. *J. Phys. Chem. B* **2003**, *107*, 5623.
- (15) Lim, M.; Jackson, T. A.; Anfirud, P. A. *Science* **1995**, *269*, 962.
- (16) Schotte, F.; Lim, M.; Jackson, T. A.; Smirnov, A. V.; Soman, J.; Olson, J. S.; Phillips, G. N., Jr.; Wulff, M.; Anfirud, P. A. *Science* **2003**, *300*, 1944.
- (17) Vojtechovsky, J.; Chu, K.; Berendzen, J.; Sweet, R. M.; Schlichting, I. *Biophys. J.* **1999**, *77*, 2153.

JA037373V